Journal of Agricultural Sciences
(Tarim Bilimleri Dergisi)

J Agr Sci-Tarim Bili
e-ISSN: 2148-9297
jas.ankara.edu.tr

# A Neural Network-Based Index (nNDVI) for Estimating the Normalized Difference Vegetation Index (NDVI) from Standard RGB Images

**İrfan Ökten[a]*, Uğur Yüzgeç[b]**

[a]*Bitlis Eren University, Faculty of Engineering and Architecture, Department of Computer Technologies, Bitlis, TÜRKİYE*
[b]*Bilecik Şeyh Edebali University, Faculty of Engineering, Computer Engineering, Bilecik, TÜRKİYE*

ARTICLE INFO
Research Article
Corresponding Author: İrfan Ökten, E-mail: iokten@beu.edu.tr
Received: 25 November 2024 / Revised: 20 May 2025 / Accepted: 02 June 2025 / Online: 30 September 2025

Cite this article
Ökten İ, Yüzgeç U (2025). A Neural Network-Based Index (nNDVI) for Estimating the Normalized Difference Vegetation Index (NDVI) from Standard RGB Images. *Journal of Agricultural Sciences (Tarim Bilimleri Dergisi),* 31(4):998-1011. DOI: 10.15832/ankutbd.1591199

ABSTRACT
An important global research topic is the analysis of the crop status, viability, and disease status of vegetables, fruits, and plants in agricultural areas. The Normalized Vegetation Difference Index (NDVI) is commonly used to analyze these conditions by using near-infrared (NIR) features in satellite images or multispectral cameras, such as Lansat-8, to produce NDVI maps. However, these methods have limitations such as high cost and difficulty in accessing images. To address these limitations, this study proposes a new neural network-based index called nNDVI, which uses a Multi-Layer Perceptron (MLP), an Artificial Neural Network (ANN), to convert the NDVI value from standard RGB images. The nNDVI allows for the analysis of vegetation in agricultural areas using low-cost RGB cameras. The MLP model was trained with R (red), G (green), and B (blue) values as input, and real NDVI values for the Swiss forest and Togo farm images were obtained with the MicaSenseAltum camera. The results of testing the model on the dataset showed an accuracy of 92.013% when comparing the nNDVI values obtained with the RGB cameras to the actual NDVI values. Thus, the proposed method demonstrates the ability to use nNDVI maps obtained using low-cost RGB cameras as an alternative to NDVI maps obtained using high-cost multispectral cameras. Overall, this study makes a valuable contribution to the field of agricultural research by presenting a cost-effective and accessible method for analyzing vegetation in agricultural areas.

Keywords: Vegetation index, NDVI, Multi-Layer Perceptron, Multi spectral camera, Agriculture

## 1. Introduction

Vegetation indices (VIs) are widely used in agricultural research, remote sensing, and environmental monitoring to assess the health, biomass, and vegetation coverage. These indices are mathematical combinations of reflectance values from different spectral bands that help distinguish vegetation from other objects such as soil, water, and built environments (Mckinnon & Hoff 2017). Through the analysis of reflectance in the visible and near-infrared (NIR) bands, vegetation indices allow for the detection of plant stress, disease, water deficiency, and overall plant vigor, as summarized in Table 1.

**Table1-Vegetative indices used for disease detection in spectroscopic studies (Sankaran et al. 2010)**

| *Vegetative Index* | *Formula* | *Reference* |
|---|---|---|
| Disease index (*fD*) | $f_D = \frac{I_{550\,nm}}{I_{550\,nm} + I_{690\,nm}}$ | Moshou & et al. (2005) |
| Normalized difference vegetation index (NDVI) | $NDVI = \frac{R_{NIR} - R_{RED}}{R_{NIR} + R_{RED}}$ | Yang & Cheng (2001), Bravo et al. (2004), Yang et al. (2007), Naidu et al. (2009) |
| Green normalized difference vegetation index (Green NDVI) | $GreenNDVI = \frac{R_{GREEN} - R_{RED}}{R_{GREEN} + R_{RED}}$ | Yang et al. (2007) |
| Water Band Index (IWB) | $I_{WB} = \frac{R_{950\,nm}}{R_{900\,nm}}$ | Xu et al. (2007) |
| Soil-adjusted vegetation index (SAVI) | $SAVI = \frac{(R_{NIR} - R_{RED})(1+L)}{R_{NIR} + R_{RED} + L}$ L=0.5 | Yang et al. (2007) |
| Photochemical reflectance index (PRI) | $PRI = \frac{R_{531\,nm} - R_{570\,nm}}{R_{531\,nm} + R_{570\,nm}}$ | Huang et al. (2010, Naidu et al. (2009) |
| Red-edge vegetation stress index (RVSI) | $RVSI = \frac{R_{714\,nm} + R_{752\,nm}}{2 - R_{733\,nm}}$ | Naidu et al. (2009) |
| Water Index (WI) | $WI = \frac{R_{900\,nm}}{R_{970\,nm}}$ | Naidu et al. (2009) |
| Visible atmospheric resistance index (VARI) | $VARI = \frac{R_{GREEN} - R_{RED}}{R_{GREEN} + R_{RED} - R_{BLUE}}$ | Naidu et al. (2009) |

*I*: *fluorescence intensity, R*: *reflectance, L: denotes a constant, which is related to the slope of the soil line in a feature-space plot.*

Normalized Difference Vegetation Index (NDVI) is one of the most widely used and studied vegetation indices (Rouse et al. 1973). The NDVI has been used for many different purposes, such as spatial referencing, crop and climate monitoring, feature mapping, and various decision support systems (Panda et al. 2010; Abdulridha et al. 2018).

Plants absorb the red band by chlorophyll and mostly reflect the Near-infrared (NIR) band. Thus, plants are separated from other materials such as soil, water, and objects (Rabetel et al. 2014). Based on this feature, the Normalized Difference Vegetation Index (NDVI) was calculated using the values in the red band and the NIR reflection to monitor plant health. Since the 1970s, the NDVI has been widely used in remote sensing to distinguish vegetation from other materials in satellite images (Sannier et al. 2002; Kumar et al. 2012). Usually, NDVI is obtained from images captured by a multispectral or hyperspectral camera that captures the correct red and NIR reflection of plants (Thenkabail et al. 2000; Deng et al. 2018; Wang et al. 2020). However, multispectral and hyperspectral cameras are heavy, expensive, and require professional operation to acquire images (Li et al. 2014).

NDVI analysis is commonly used in agriculture worldwide to monitor drought, predict agricultural productivity, detect if plants are sick, detect vegetation destruction in fire zones, etc.. An NDVI map of a terrain or location can be obtained from satellite images via remote sensing, or from an unmanned aerial vehicle equipped with a multispectral sensor operating at the NIR wavelength. Obtaining these values instantly from satellite images is costly and depends on weather conditions. Acquiring an NDVI map with a multispectral sensor integrated into a drone is a more effective method. However, multispectral cameras are much more expensive than standard RGB-based cameras, and the calibration processes take time to be ready for use. Currently, high-resolution conventional RGB cameras are available from different manufacturers, and most Unmanned Aerial Vehicles (UAVs) are equipped with these RGB cameras (Rabatel et al. 2011). Therefore, it is possible to come across studies in the literature suggesting different plant indices with approximately the same performance as an alternative to these expensive methods.

Costa et al. (2020) estimated NDVI using RGB images with a genetic algorithm for three different crops (citrus, grapes, and sugarcane). Using this method, they obtained an average error of 0.052 and average error rate of 6.89%. Picon et al. (2022) proposed an end-to-end method for powerful vegetation segmentation via RGB images that can divide vegetation appropriately without the need for an infrared-capable camera, even under vegetation-damaged conditions. They used a convolutional semantic regression network to predict a virtual near-infrared channel from an RGB image (RGB2NIR). They obtained values of R=0.93, MAE = 0.05. Rabatel et al. (2011) replaced the near-infrared blocking filter in the NIR and R bands, which is required to calculate NDVI, with a low-pass filter. As a result of this change, they showed that NDVI can be achieved NDVI with an RGB-based camera. Wang et al. (2020) have integrated a NIR sensitive sensor into a Raspberry Pi with RGB camera. This integrated sensor is much more affordable than multispectral cameras. They achieved high performance ($R^2$ = 0.96, RMSE = 0.0079) in estimating the real NDVI value and NDVI values using the proposed method. Houborg & McCabe (2016) used NDVI and RGB images from Planet Labs from Lansat-8 satellite images and converted them using cubist regression, which is a data mining method. Using this method, they obtained an $R^2$ value of 0.97. Arai et al. (2016) found a high correlation between NIR reflectance and green colour reflection. Therefore, it has been suggested that it is possible to estimate the NIR reflectance using visible camera data.

They used green reflection instead of NIR to obtain the NDVI values. For plant phenotyping, indices to assess plant water status, phytosanitary status, or water stress and for disease detection, various vegetation indices (VIs) have been developed from data collected by UAV [26,27,28] (Ampatzidis et al. 2017; Abdulridha et al. 2019; Abdulridha et al. 2020). Ayhan et al. (2020) performed vegetation detection using CNN and DeepLabV3, which are deep learning methods. However, at the end of the experiments, they determined that it was more successful in detecting vegetation using computer vision and machine learning with NDVI, without training. In their study, Adamiak et al. (2022) discussed and validated the potential of using conditional generative adversarial networks (cGAN) to perform image-to-image translation that can predict NDVI from a single panchromatic orthoimage.

Similarly, Davidson (2021) investigated the use of artificial intelligence, specifically a conditional Generative Adversarial Network (Pix2Pix), to predict NDVI and the Normalized Difference Red Edge Index (NDRE) from standard RGB aerial imagery. This approach offers a cost-effective solution by eliminating the need for expensive multispectral cameras, thus making vegetation index estimation more accessible for precision agriculture applications.

There are four sections in the remainder of the study. In the materials and methods in the 2nd section, basic information about NDVI and MLP is provided. In the third section, information about the multispectral dataset used in the study and how the dataset is generated from these multispectral images for the MLP model is presented. The training and test results of the proposed MLP model are presented in section 4. In the last section, the general results of these studies are presented.

## 2. Material and Methods

This study proposes an MLP model to develop a new neural-network-based index (nNDVI) for predicting NDVI values from standard RGB images. The MLP model uses three inputs (R, G, and B) and produces one output (nNDVI) with a structure of three hidden layers. For model training and evaluation, MicaSenseAltum multispectral data including six spectral bands were used. A total of 40 multispectral images were employed for training and 10 separate images were used for testing. The model achieved a mean squared error (MSE) of 0.036, demonstrating high accuracy in NDVI estimation from the RGB data.

The main contributions of this study are as follows:

1- The development of a cost-effective and accessible neural-network-based index (nNDVI) to estimate NDVI using standard RGB cameras provides an alternative to expensive multispectral or hyperspectral systems.

2- The high accuracy of the MLP model in predicting NDVI values highlights its potential for agricultural monitoring and vegetation analysis.

In summary, this study presents a promising approach for NDVI estimation from RGB images, addressing the key limitations of current multispectral-based methods and enhancing accessibility for agricultural research and practice.

### *2.1. Normalized Difference Vegetation Index (NDVI)*

A healthy plant absorbs red and blue light through chlorophyll and reflects green light. Therefore, a healthy plant appears green. Plants reflect NIR beams as well as green visible light, and the healthier the plant, the more NIR beams it will reflect. When a plant is dehydrated or stressed, its leaves reflect less near-infrared light. To understand the health of a plant, the reflection values of the Red and NIR rays should be compared. The Normalized Difference Vegetation Index (NDVI) measures the difference between near infrared and red light, giving information about the state of vegetation. The NDVI value was calculated using the NIR and Red bands of satellite images or multispectral cameras as follows [17]:

$$NDVI = \frac{R_{NIR} - R_{Red}}{R_{NIR} + R_{Red}} \quad (1)$$

Where; $R_{NIR}$ represents the reflectance of the *NIR* band and $R_{Red}$ represents the reflectance of the red band. NDVI maps were created as a result of the analysis of NDVI values obtained from multispectral cameras. Satellite sensors, such as Landsat and Sentinel-2, have the required NIR and red bands. The NDVI values range from -1 to +1. There is no separate lower limit for each land cover type in this range. Negative NDVI values indicate the presence of water. NDVI values close to +1 most likely indicated green-leaved plants. NDVI is a standard method for measuring healthy vegetation. High NDVI values indicate that the plant is healthy, whereas low values indicate unhealthy conditions or problems in the plant. Based on the results of the NDVI analysis, the ranges shown in Figure 1 were used for plant phenotyping.


**Figure 1- State of the plant according to the NDVI value ranges**

*2.2. Multilayer Perceptron (MLP)*

Multilayer Perceptron (MLP) networks are a type of artificial neural network that includes at least one hidden layer between the input and output layers, enabling them to solve nonlinear problems, unlike single-layer perceptrons (Arıkan Kargı 2014). An MLP typically consists of an input layer, one or more hidden layers, and an output layer (Dhamija & Bhalla 2011). The input layer contains neurons representing independent variables, hidden layers capture nonlinear relationships, and the output layer generates the model's predictions (Baranoff et al. 2000).

MLPs operate through forward propagation, where input data pass through the network to generate an output, and backpropagation, where errors are propagated backward to adjust the weights of the model and minimize the prediction errors. Each hidden neuron applies a nonlinear activation function to the weighted sum of its inputs and bias term (Trenn 2008). Figure 2 illustrates an MLP model with three inputs, three hidden layers, and one output.

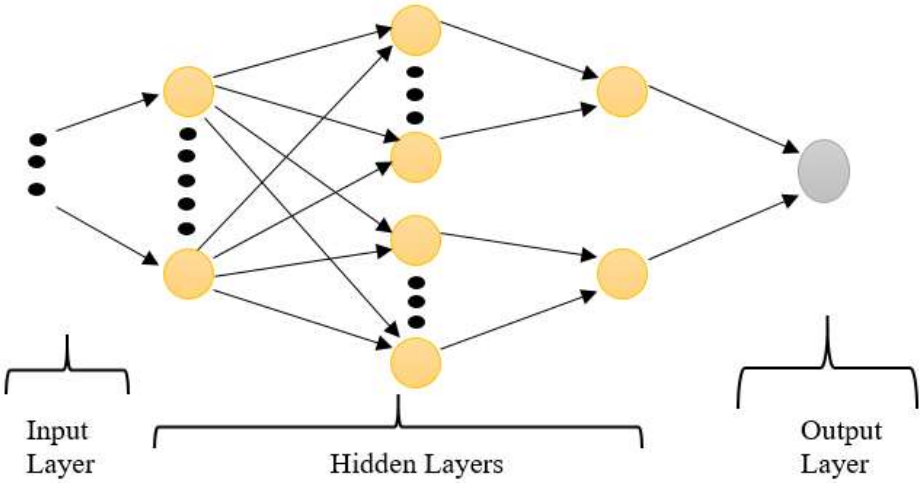


**Figure 2- MLP model with three inputs and one output consisting of three hidden layers**

The working structure of multilayer perceptrons consists of two stages: forward computation, where the output of the network is calculated, and backward computation, where the weights are updated. The main purpose of forward calculation is to estimate the output value for the given input values and calculate the error using the target value (Murtagh 1991).

*2.3. A Neural Network-Based Normalized Difference Vegetation Index (nNDVI)*

In this study, an MLP model (Figure 3) was designed to estimate NDVI values from RGB images by introducing a new neural-network-based vegetation index, nNDVI. The model uses red, green, and blue channel values as inputs and predicts the nNDVI value as the output. Pixel-level R, G, and B values from each image were used as input data to estimate the corresponding NDVI values.

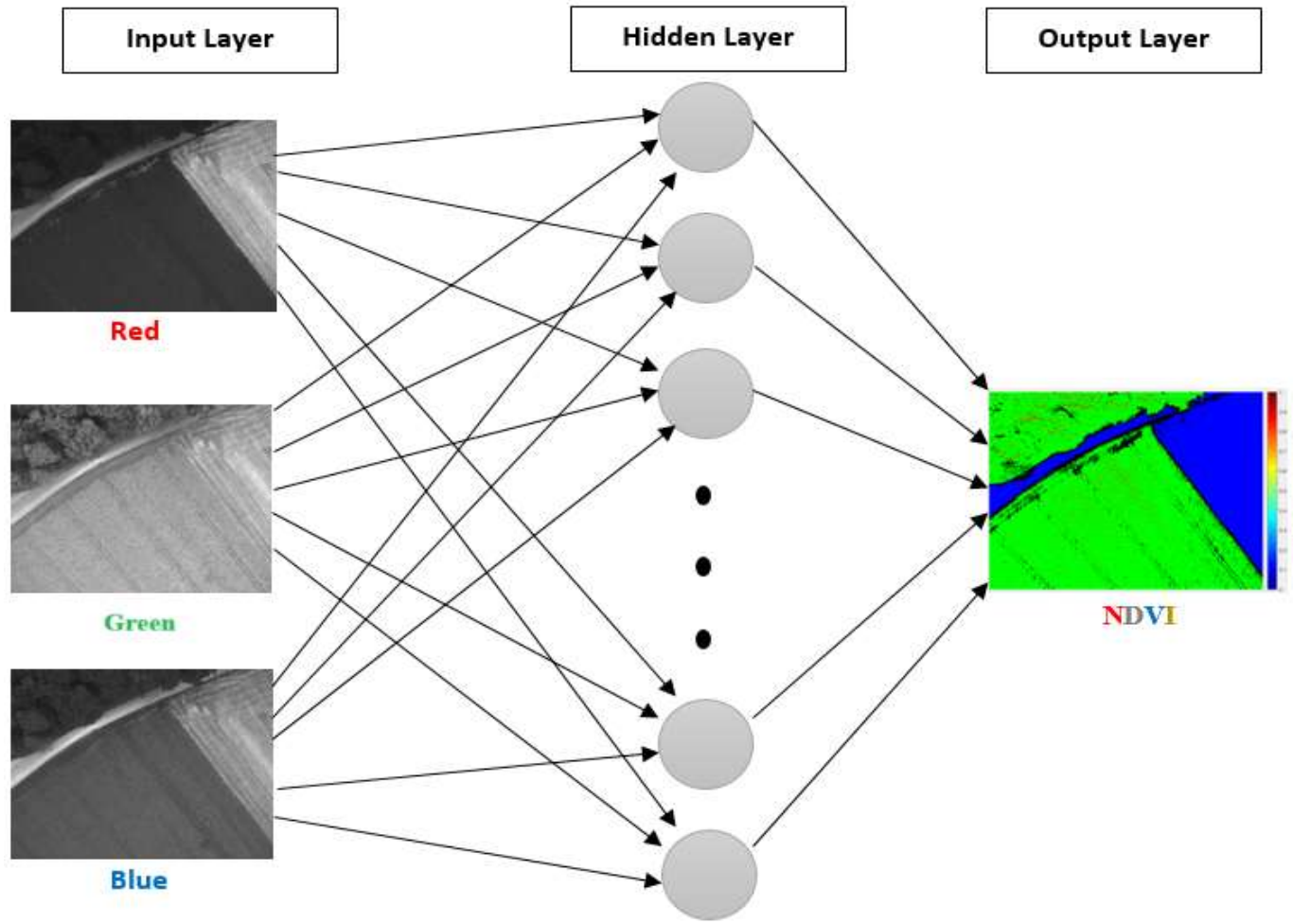


**Figure 3-A Proposed MLP model for NDVI estimation from RGB images**

The numbers of hidden layers and neurons in the proposed MLP model were determined using a trial-and-error approach. As shown in Figure 4, the final model consisted of three inputs (R, G, and B), three hidden layers, and one output (nNDVI). The hidden layers included eight, thirteen, and nine neurons. To evaluate the model, the RGB2NDVI dataset was split into 70% training, 15% validation, and 15% testing.

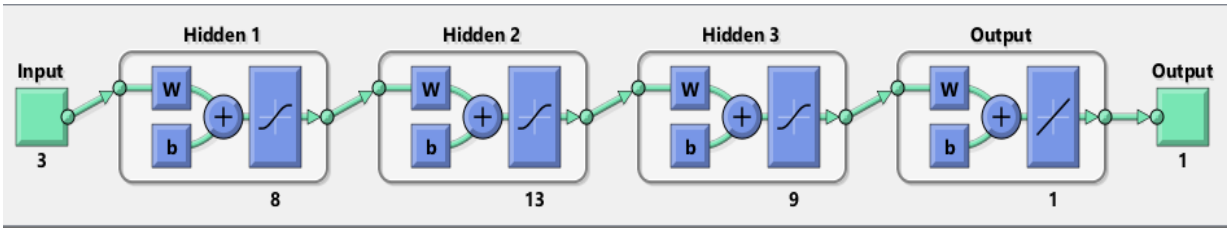


**Figure 4-MLP model with three inputs (R, G, and B) and one output (nNDVI)**

*2.4. Evaluation metrics*

Evaluation metrics are important tools for measuring and evaluating model performance. In machine learning and statistics, various metrics are used to understand how well a model performs and compare different models. These metrics show how accurate the model's predictions are, how reliable they are, and what kinds of errors they make. In this study, RMSE and MSE evaluation metrics were used.

*2.5. MSE (Mean Squared Error)*

The MSE is the mean of the squared differences between the predicted and true values. In other words, we squared the prediction error for each data point and calculated the mean of these squares. The MSE measures the magnitude of the errors in the model's

predictions, and higher MSE values indicate worse performance of the model. It is sensitive to outliers because squaring magnifies the effects of large errors. The formula for MSE is as follows:

$$MSE = \frac{1}{n}\sum_{i=1}^{n}(y_i - \hat{y}_i)^2 \quad (2)$$

Where; $n$ is the number of data points, $y_i$ is the predicted values, and $\hat{y}_i$ is the actual values.

*2.6. RMSE (Root Mean Squared Error)*

RMSE is the square root of the MSE. It carries the same information as MSE but expresses the error values in their original units. This makes the RMSE easier to interpret because it shows the magnitude of the error on the scale of the target variable. For example, if you are making temperature forecasts, the RMSE indicates how many degrees the forecast error is, on average. RMSE is as sensitive to outliers as MSE. The RMSE is calculated as follows:

$$RMSE = \sqrt{\frac{1}{n}\sum_{i=1}^{n}(y_i - \hat{y}_i)^2} \quad (3)$$

*2.7. Dataset*

*2.7.1. RGB and multispectral dataset*

A raw image dataset from multispectral cameras was required for the proposed RGB2NDVI model. Multispectral cameras are neither ubiquitous nor inexpensive. To train and test this model, data obtained with a camera that captures images in the Red, Green, Blue and NIR bands of the same region are required. Therefore, a free dataset is obtained using Wingtra. In this study, we used data obtained from MicaSenseAltum, a multispectral camera available on the Wingtra website (Switzerland 2022).

Two regional datasets were used from the multispectral data presented by Wingtra. In the first region, Switzerland, 50 hectares of farmland were mapped using the WingtraOne Micasense Altum system. Maps were created with a GSD of 4.0 cm/px in the multispectral layers and 61 cm/px in the thermal LWIR layer (flight altitude of 90 m AGL). The bands of the sample image obtained from agricultural land in Switzerland are shown in Figure 5. The second region, Togo, was mapped using the WingtraOne MicasenseAltum system on a 210-hectare farm (Togo 2022). Maps were created with a GSD of 9.0 cm/px in multispectral layers. The bands of a sample image obtained from the farm field in Togo are shown in Figure 6.

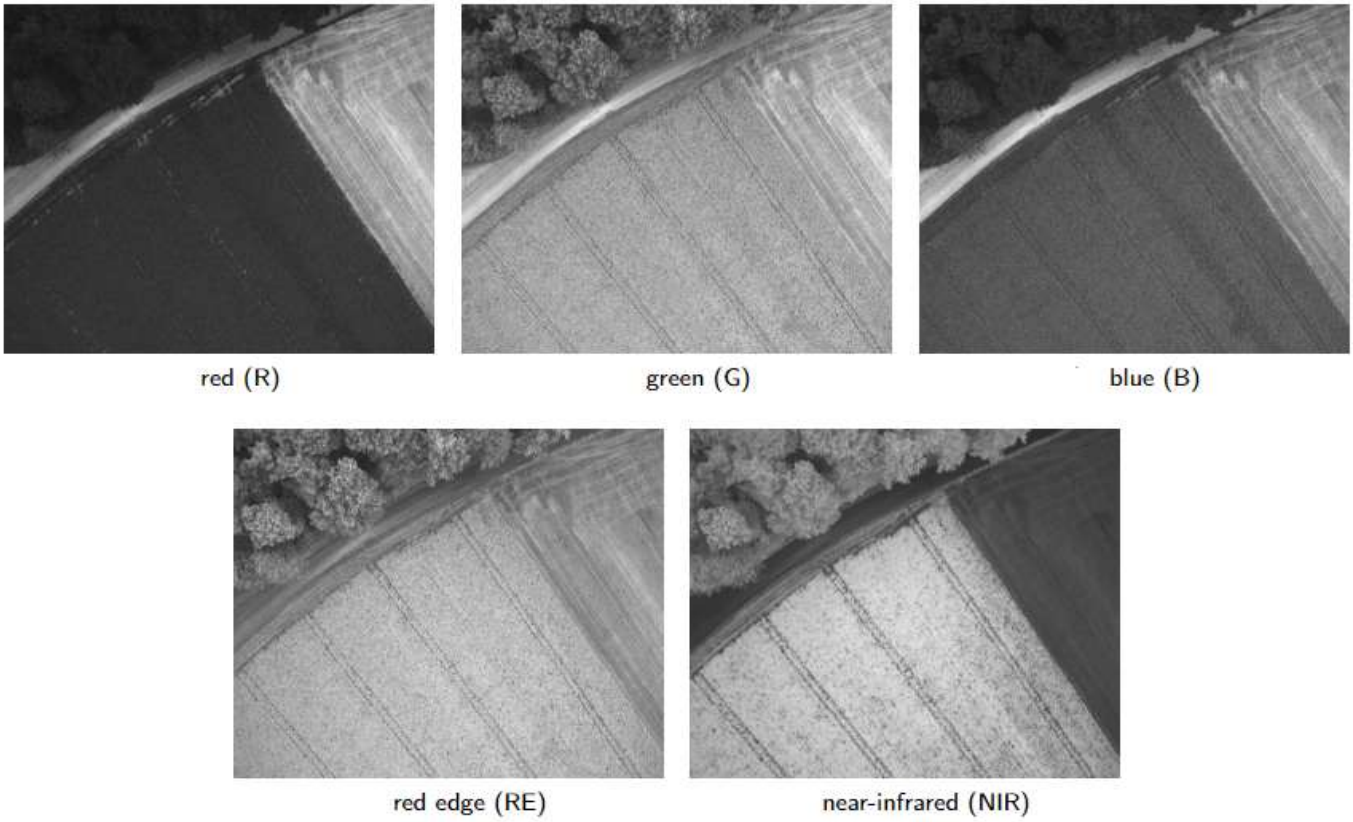


**Figure 5- Multispectral sample data (agricultural fields in Switzerland)**

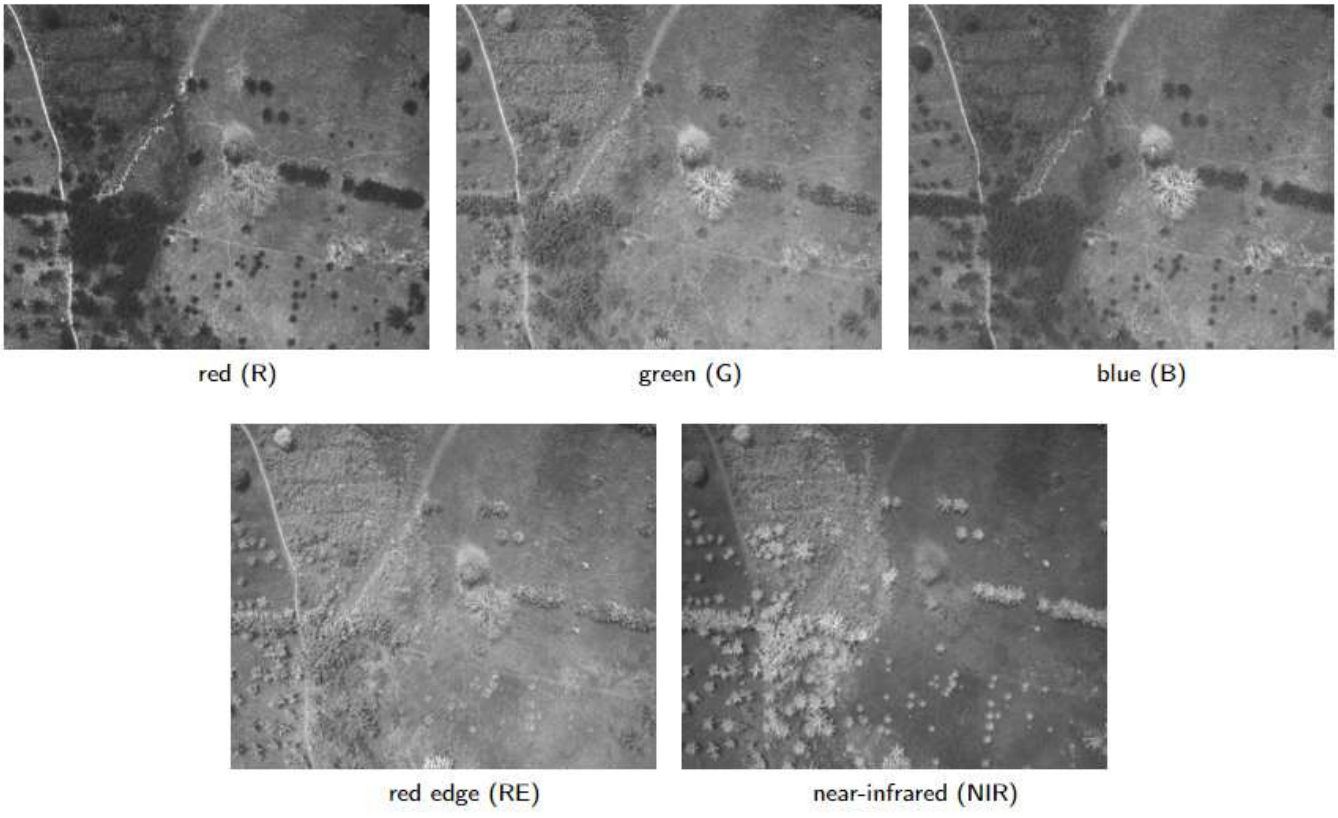


**Figure 6- Multispectral sample data (Farm in Togo)**

By combining the red, green, and blue band values from the 5-channel images taken from the multispectral dataset, the RGB image is obtained, and the NDVI image is obtained using Eq.1 from the red and NIR band values. Figure 7 shows the RGB, raw NDVI, and colored NDVI images obtained from the multispectral dataset used in this study.

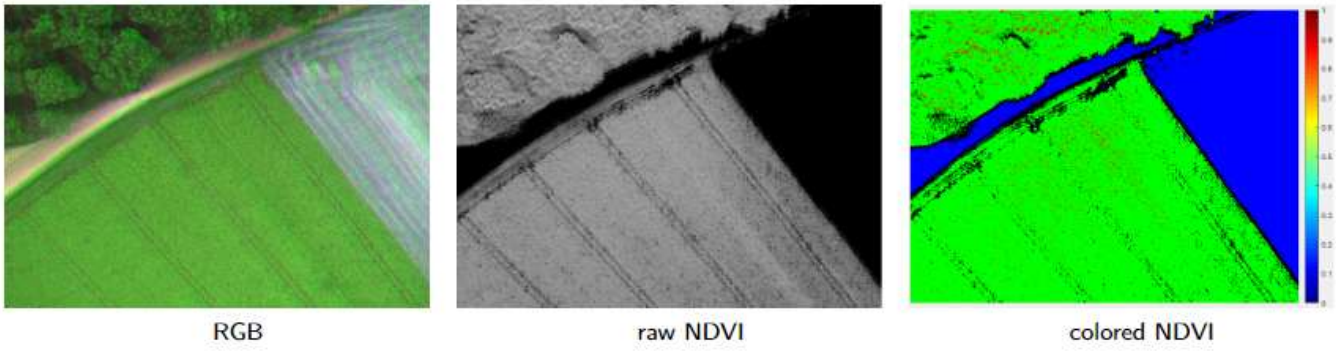


**Figure 7- RGB, raw NDVI, and colored NDVI images from multispectral data**

*2.8. Creating the dataset*

In this subsection, the images in the dataset described in the data collection section are adapted to the use of the MLP model. Red, green, and blue band values were assigned to the input of the MLP model to determine the nNDVI value. A MATLAB script was written to generate a raw and colored NDVI map from RGB data. In model training, the NDVI data were calculated for each dataset and used as the target values in the model output. Figure 8 shows how to create a dataset to be used in the training and testing stages of the MLP model from multispectral data.

A dataset was created for use in the training and testing stages of the proposed MLP model to predict NDVI data from standard RGB images. As can be seen in Figure 8, the size of each image added to the input dataset from the multispectral images taken was 1,228,800 (1280 × 960 × 1) pixels in total. This pixel value also indicates the size of each input data point to be assigned to the MLP model. Because the proposed MLP model has three inputs (R, G, and B), the RGB data were converted into a three-column matrix (1,228,800 × 3) with a script written in MATLAB. For each multispectral image added to the dataset, the RGB data were added to the input matrix as a three-column matrix. To obtain the output dataset, NDVI values were calculated using the red and NIR bands from the multispectral data.

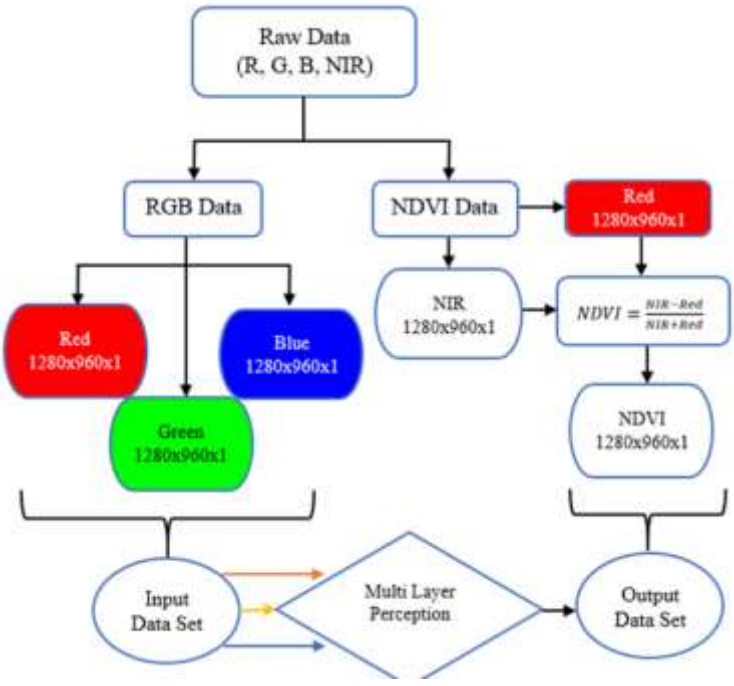


**Figure 8- Input and output dataset creation scheme**

Table 2 summarizes the information from the RGB2NDVI dataset created for use in the proposed MLP model to estimate the NDVI value. Table 3 shows some sample values of 49,152,000 datasets consisting of 40 images used for training the model.

**Table 2-RGB2NDVI dataset information for MLP model**

| *Number of images* | *Input matrix size [Red; Green; Blue]* | *Output matrix size [NDVI]* | *Dataset Size* |
|---|---|---|---|
| 1 image | [1228800; 1228800; 1228800] | [1228800] | 1280x960x1=1228800 |
| 40 images | [49152000; 49152000; 49152000] | [49152000] | 1280x960x40=49152000 |

**Table 3- Some RGB2NDVI dataset pixel values**

| ***Number of datasets*** | ***Red value*** | ***Green value*** | ***Blue value*** | ***Calculated NDVI value*** |
|---|---|---|---|---|
| 1 | 0.2017 | 0.1887 | 0.6624 | 0.4449 |
| . | - | - | - | - |
| . | - | - | - | - |
| 816,341 | 0.2302 | 0.2927 | 0.5134 | 0.2684 |
| 816,342 | 0.1821 | 0.2915 | 0.4856 | 0.3549 |
| 816,343 | 0.2094 | 0.2905 | 0.5087 | 0.2741 |
| 816,344 | 0.1796 | 0.2695 | 0.4890 | 0.3437 |
| . | - | - | - | - |
| . | - | - | - | - |
| 49,152,000 | 0.2376 | 0.5601 | 0.3042 | 0.4338 |

## 3. Results and Discussion

In this section, the training results of the MLP model that estimated the NDVI values are presented. Then, tests of the model were carried out with different test images that were not included in the training set. The dataset prepared for training the MLP model consisted of 40 images of 1280x960 sizes. The red, green, and blue bands in this dataset are the inputs to the MLP model. The target NDVI values at the output of the model were obtained using the NIR and red band values in the dataset.

There are several training methods for optimizing the parameters of a neural network model. In the first stage, we discuss the training methods. A comparison of the results of the standard neural network training methods for the nNDVI estimation model is presented in Table 4. The training methods used in this table are the Levenberg-Marquardt (LM), BFGS quasi-Newton (BFG), Resilient Backpropagation (RP), Scaled Conjugate Gradient (SCG), Conjugate Gradient with Powell-Beale restarts (CGB), Conjugate Gradient with Fletcher-Reeves (CGF), Conjugate Gradient with Polak-Ribie´re (CGP), One-Step Secant (OSS), Gradient Descent with momentum and adaptive learning rate (GDX).

**Table 4- Comparison results of training functions for the nNDVI estimation model**

| *Training Method* | *Test Accuracy Rate (%)* | *Training Method* | *Test Accuracy Rate (%)* |
|---|---|---|---|
| LM | 92.013 | CGB | 91.870 |
| BFG | 91.875 | CGF | 91.687 |
| RP | 91.122 | CGP | 91.215 |
| SCG | 91.770 | OSS | 91.416 |
| GDX | 87.515 | | |

To obtain the results in this table, the weight parameters of the proposed nNDVI estimation model were optimized using each training method, and then the accuracy rates of the model were determined for the test data. As shown in Table 4, the best accuracy rate was obtained for the LM (Levenberg-Marquardt) training method. As can be seen from these results, the LM method was used for parameter optimization of the proposed nNDVI estimation model.

The correlations between the nNDVI predictive values obtained with the proposed MLP model and the actual NDVI values for training, validation, testing, and all phases are shown in Figure 9.

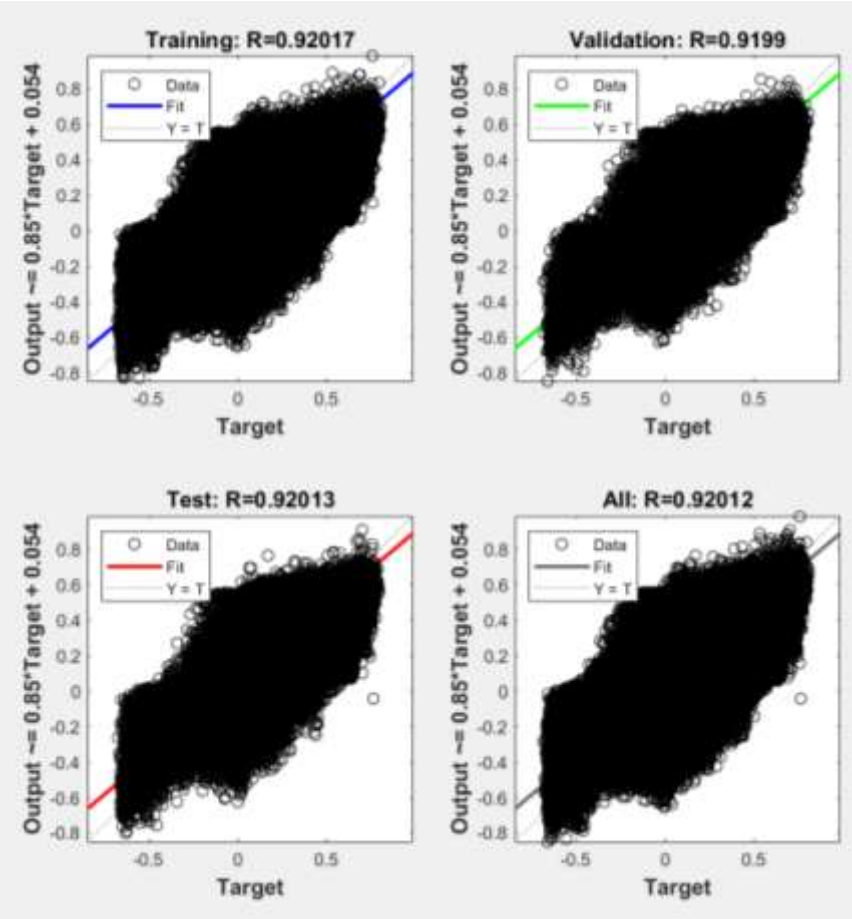


**Figure 9- Regression curves of the nNDVI estimation model: R=92.017 for training, R=91.999 for validation, R=92.013 for testing, and R=92.012 for all stages**

In these figures, target labels represent the real NDVI data, output labels represent the output of the nNDVI estimation model. In these correlation results, data of 34,406,400 pixels were used for the training stage and 7,372,800 pixels for the validation and testing stages. However, due to the large dataset used, the interpretation of the regression plots became difficult. The graphical results of 44-pixel values selected randomly from the dataset used to compare the nNDVI estimation values and real NDVI values are shown in Figure 10. As can be seen from these figures, it is clearly seen that there is a good correlation between the nNDVI produced by the model estimating the NDVI data from the standard RGB image and the actual NDVI value calculated from the multispectral data.

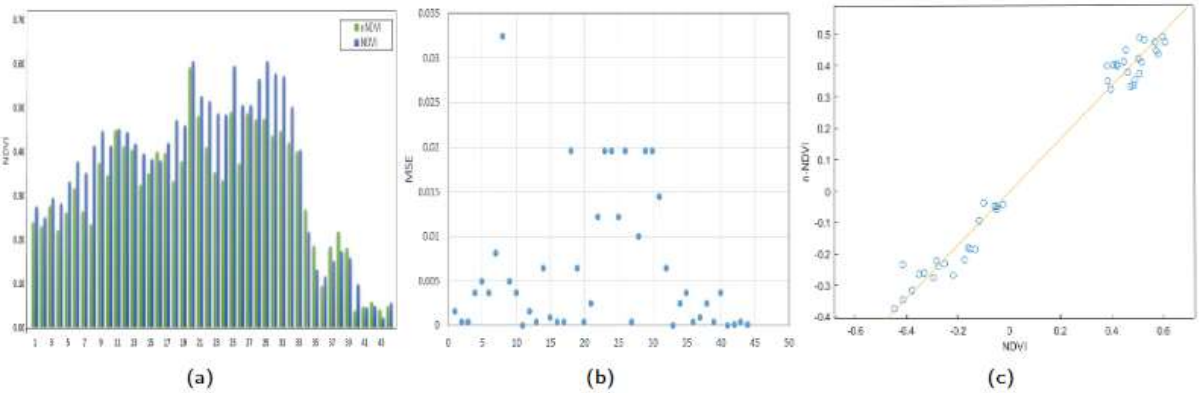


**Figure 10- (a) Test comparison between nNDVI and NDVI, (b) MSE for each pixel, and (c) correlation between nNDVI and NDVI for 44 random pixels from an image in the dataset**

To evaluate the proposed MLP model for estimating the NDVI value, we used 10 different multispectral images from the dataset that were not used in the training phase. The output nNDVI data were obtained by applying the red, green, and blue bands of these images to the trained network model. The nNDVI results obtained for the three images from the multispectral dataset

are shown in Figure 11. These subfigures consist of the estimated raw nNDVI images, original raw NDVI images, original colored NDVI images, and the estimated colored nNDVI images for the three test images. To measure the performance of the nNDVI estimation model in the test results, the Mean Squared Error (MSE) and Root Mean Squared Error (RMSE) were calculated for each test image. The results are summarized in Table 5.

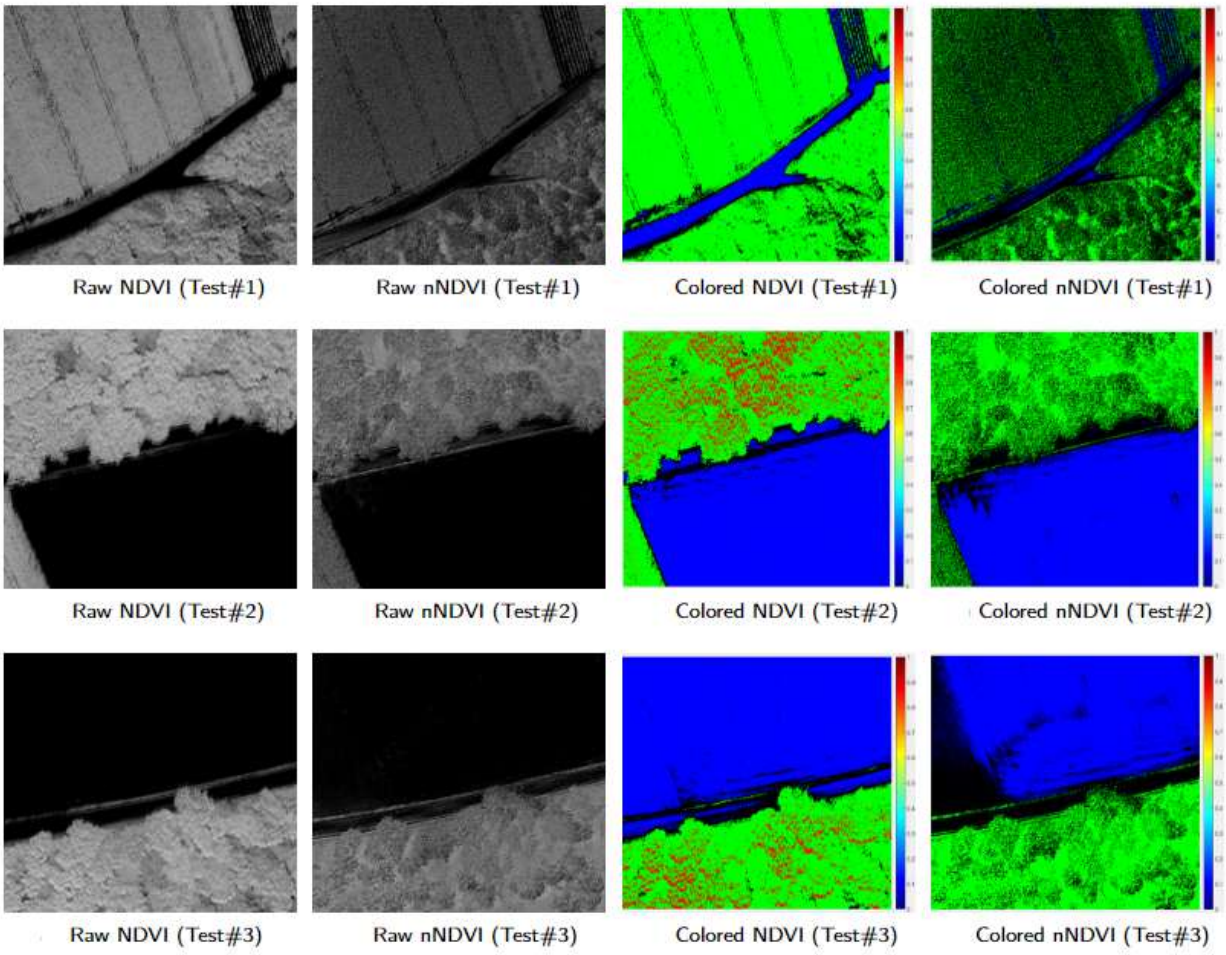


**Figure 11- Comparison test results of nNDVI estimated from RGB and NDVI from multispectral data**

**Table 5- MSE and RMSE results of the test images**

| *Test No* | *MSE* | *RMSE* |
|---|---|---|
| Test #1 | 0.0532 | 0.2307 |
| Test #2 | 0.0356 | 0.1888 |
| Test #3 | 0.0258 | 0.1607 |
| Test #4 | 0.0260 | 0.1611 |
| Test #5 | 0.0347 | 0.1862 |
| Test #6 | 0.0180 | 0.1342 |
| Test #7 | 0.0359 | 0.1895 |
| Test #8 | 0.0277 | 0.1664 |
| Test #9 | 0.0794 | 0.2817 |
| Test #10 | 0.0236 | 0.1537 |

The mean MSE value of the nNDVI estimation model for the ten test images was 0.036, and the mean RMSE value was 0.1853. The error metrics in this table show that the proposed neural network-based index (nNDVI) to estimate NDVI data from RGB data can be a helpful alternative to multispectral cameras.

### *3.1. Comparison with existing NDVI estimation methods*

The proposed neural network-based index (nNDVI) was compared with existing approaches in the literature to estimate the NDVI from RGB images. Costa et al. (2020) used a genetic-algorithm-based method and achieved an average error of 0.052 and an error rate of 6.89%. Although effective, genetic algorithms require high computational effort, whereas our MLP-based model achieved a lower mean squared error (MSE) of 0.036 and 92.013% accuracy, offering a more efficient solution.

Rabatel et al. (2014) estimated NDVI by modifying camera filters to capture NIR data indirectly. However, this approach requires hardware modifications, which limit its practical use. In contrast, our model works directly with unmodified RGB images, thereby increasing its applicability in real-world agricultural scenarios.

Additionally, Picon et al. (2022) proposed a deep convolutional neural network (CNN) to predict NIR channels from RGB images, achieving a correlation (R) of 0.93 and an MAE of 0.05. Although successful, CNN-based models are computationally demanding and require large datasets. Our simpler MLP model achieved comparable accuracy without such requirements, making it more practical for field applications.

Finally, Houborg & McCabe (2016) used cubist regression to estimate NDVI from RGB images with $R^2 = 0.97$, but this method often requires manual tuning. In contrast, MLP models, such as ours, learn complex patterns automatically from the data.

As a result, the proposed nNDVI model provides a cost-effective, accessible, and accurate alternative to existing methods for estimating NDVI from RGB images, making it particularly suitable for agricultural monitoring where low-cost and efficient solutions are required (Rabatel et al. 2011; Houborg & McCabe 2016; Costa et al.2020; Picon et al. 2022).

### *3.2. Real-time applicability and environmental factors*

The feasibility of deploying the proposed nNDVI model in real-time drone applications depends on the computational efficiency and processing time. In drone-based remote sensing, the onboard processing capabilities are often limited, necessitating lightweight models or external ground-based processing. Our nNDVI model, based on MLP, has a relatively low computational cost compared to deep learning architectures, making it suitable for real-time or near-real-time applications.

To assess real-time feasibility, we evaluated the average processing time of the nNDVI estimation on a workstation equipped with an Intel Core i7 processor and an NVIDIA RTX 3060 GPU. The model processed a 1280×960 image in approximately 1 s. For embedded systems such as NVIDIA Jetson or Raspberry Pi, the processing time is expected to be higher owing to hardware constraints; however, further optimizations, such as model quantization or GPU acceleration, could improve performance. Future work will focus on directly deploying and testing the model on UAV platforms to validate its operational efficiency under field conditions.

Another critical factor affecting the reliability of nNDVI is the effect of varying lighting conditions and shadows. Unlike the traditional NDVI, which utilizes near-infrared reflectance, RGB-based indices are more susceptible to illumination changes. In outdoor environments, variations in sunlight intensity, cloud cover, and object shadows can lead to inconsistencies in RGB values, thereby affecting nNDVI predictions. To mitigate these effects, preprocessing techniques, such as histogram equalization, white balance correction, or adaptive exposure adjustments, can be applied before feeding the images into the model. Additionally, integrating multiple images captured under different lighting conditions during training can improve the robustness of the model.

Future research should focus on incorporating shadow detection and compensation algorithms to further enhance the reliability of the nNDVI under dynamic environmental conditions. Implementing real-time adjustments based on ambient lighting sensors or high dynamic range (HDR) imaging techniques could also provide more stable estimations across different times of the day and varying weather conditions.

## 4. Conclusions

The use of Normalized Difference Vegetation Index (NDVI) maps for crop assessment, viability, and disease detection is a well-established agricultural research topic. However, generating these maps using methods such as satellite images or multispectral cameras poses several challenges, including high cost and limited accessibility. Furthermore, the effectiveness of remote-sensing-based methods is often affected by adverse weather conditions, such as cloud cover. As an alternative, multispectral cameras mounted on drones or Unmanned Aerial Vehicles (UAVs) have been utilized to create NDVI maps in agricultural areas. However, the cost of these camera systems is still comparatively high, limiting their widespread adoption.

To address this issue, a new neural network-based index (nNDVI) is proposed in this study, which utilizes a Multi-Layer Perceptron (MLP) model with three hidden layers to estimate NDVI values from RGB images. The proposed nNDVI was shown to accurately predict NDVI values obtained from multispectral cameras in ten test images taken from MicaSenseAltum, with an

average mean squared error (MSE) of 0.036 and root mean squared error (RMSE) of 0.1853. This new method allows the production of NDVI maps of agricultural lands using low-cost RGB cameras mounted on drones.

Future research should aim to develop pre-trained Convolutional Neural Network (CNN) models for the early detection of rice plant diseases by converting images of rice plant leaves taken with an RGB camera to nNDVI values. The proposed nNDVI estimation model with a standard RGB camera can serve as an alternative to NDVI data for various agricultural products. Furthermore, the estimation of NDVI from RGB data can be further improved in future studies by exploring alternative models and methods.

**Contributions of the Authors**

IO: Conceptualization, Methodology, Writing, Data Preparation, Software. UY: Supervision, Writing, Review, Editing.

**Conflict of Interest Statement**

The authors declare that they have no conflicts of interest.

**Statement of Research and Publication Ethics**

This study complied with research and publication ethics.

## References


Abdulridha J, Ampatzidis Y, Ehsani R & de Castro A I (2018). Evaluating the performance of spectral features and multivariate analysis tools to detect laurel wilt disease and nutritional deficiency in avocado. Comput. Electron. Agric. 155: 203–211. https://doi.org/10.1016/j.compag.2018.10.016.

Abdulridha J, Ampatzidis Y, Kakarla S C & Roberts P (2020). Detection of target spotand bacterial spot diseases in tomato using UAV-based and benchtop-based hyperspectral imaging techniques. *Precision Agriculture* 21(5): 955–978. https://doi.org/10.1007/s11119-019-09703-4

Abdulridha J, Ehsani R, Abd-Elrahman A &Ampatzidis Y (2019). A remote sensing technique for detecting laurel wilt disease in avocado in presence of other biotic and abiotic stresses. *Computers and Electronics in Agriculture*, *156*, 549–557. https://doi.org/10.1016/j.compag.2018.12.018

Adamiak M, Będkowski K &Bielecki A (2022). *Generative adversarial approach to urban areas ndvi estimation using information exclusively from structural and textural analysis of panchromatic orthoimagery: A case study of Łódź*.

Agricultural field in Switzerland (processed), MicaSenseAltum, 48ha, 4cm/px - Google Drive, Google.com. [Online]. Available: https://drive.google.com/drive/folders/1HsM6NoFMtJIhh-SmxjnYHyRcVuAx3535. [Accessed: 12-Apr-2022].

Ampatzidis Y, De Bellis L &Luvisi A (2017). IPathology: Robotic applications and management of plants and plant diseases. Sustainability, 9(6), 1010. https://doi.org/10.3390/su9061010

Arai K, Gondoh K, Shigetomi O & Yuko (2016). Method for NIR reflectance estimation with visible camera data based on regression for NDVI estimation and its application for insect damage detection of rice paddy fields. *International Journal of Advanced Research in Artificial Intelligence*, *5*(11). https://doi.org/10.14569/ijarai.2016.051103

Arıkan Kargı V S (2014). "A comparison of artificial neural networks and multiple linear regression models as in predictors of fabric weft defects", Tekstil ve Konfeksiyon, 24, 309-316

Ayhan B, Kwan C, Budavari B, Kwan L, Lu Y, Perez D, Li J, Skarlatos D & Vlachos M (2020). Vegetation detection using deep learning and conventional methods. *Remote Sensing*, *12*(15), 2502. https://doi.org/10.3390/rs12152502

Baranoff E G, Sager T W & Shively T S (2000). A semiparametric stochastic spline model as a managerial tool for potential insolvency. *The Journal of Risk and Insurance* 67(3), 369. https://doi.org/10.2307/253834

Bravo C, Moshou D, Oberti R, West J, Mccartney A, Bodria L & Ramon H (2004). Foliar disease detection in the field using optical sensor fusion. *Agricultural Engineering International: The CIGR Journal of Scientific Research and Development*.

Costa L, Nunes L &Ampatzidis Y (2020). A new visible band index (vNDVI) for estimating NDVI values on RGB images utilizing genetic algorithms. *Computers and Electronics in Agriculture*, *172*(105334), 105334. https://doi.org/10.1016/j.compag.2020.105334

Davidson M W (2021). *Deeplearning-basedestimation of NDVI and NDRE from RGB aerialimageryusingconditionalgenerativeadversarialnetworks (Pix2Pix)*. University of Illinois. Retrieved from https://www.ideals.illinois.edu/items/121068

Deng L, Mao Z, Li X, Hu Z, Duan F & Yan Y (2018). UAV-based multispectral remote sensing for precision agriculture: A comparison between different cameras. *ISPRS Journal of Photogrammetry and Remote Sensing: Official Publication of the International Society for Photogrammetry and Remote Sensing (ISPRS)*, 146, 124–136. https://doi.org/10.1016/j.isprsjprs.2018.09.008

Dhamija A K & Bhalla V K (2011). Exchange rate forecasting: comparison of various architectures of neural networks. *Neural Computing & Applications* 20(3): 355–363. https://doi.org/10.1007/s00521-010-0385-5.

Huang M & Lu R (2010). Apple mealiness detection using hyperspectral scattering technique. *Postharvest Biology and Technology*, *58*(3), 168–175. https://doi.org/10.1016/j.postharvbio.2010.08.002

Houborg R & McCabe M (2016). High-resolution NDVI from Planet's constellation of earth observing nano-satellites: A new data source for precision agriculture. *Remote Sensing*, *8*(9), 768. https://doi.org/10.3390/rs8090768

Kumar A, Bhandari A K & Padhy P (2012). Improved normalised difference vegetation index method based on discrete cosine transform and singular value decomposition for satellite image processing. *IET Signal Processing*, *6*(7), 617. https://doi.org/10.1049/iet-spr.2011.0298

Li L, Zhang Q & Huang D (2014). A review of imaging techniques for plant phenotyping. *Sensors (Basel, Switzerland)*, *14*(11), 20078–20111. https://doi.org/10.3390/s141120078

Mckinnon T & Hoff P (2017). Comparing RGB-based vegetation indices with NDVI for drone based agricultural sensing. Agribotix. Com 1–8.

"Model Farm in Togo, MicaSenseRedEdge-M, 210 ha, 9 cm/px - Google Drive," Google.com. [Online]. Available: https://drive.google.com/drive/folders/1qtMXZCDk_rRglrACGO-V9WOwxZJI3bxS. [Accessed: 12-Apr-2022].

Moshou D, Bravo C, Oberti R, West J, Bodria L, Mccartney A & Ramon H (2005). Plant disease detection based on data fusion of hyper-spectral and multi-spectral fluorescence imaging using Kohonen maps Real-Time Imaging. 11: 75–83

Murtagh F (1991). Multilayer perceptrons for classification and regression. *Neurocomputing*, 2(5–6): 183–197. https://doi.org/10.1016/0925-2312(91)90023-5

Naidu R A, Perry E M, Pierce F J & Mekuria T (2009). The potential of spectral reflectance technique for the detection of Grapevine leafroll-associated virus-3 in two red-berried wine grape cultivars. *Computers and Electronics in Agriculture*, *66*(1), 38–45. https://doi.org/10.1016/j.compag.2008.11.007

Panda S S, Ames D P & Panigrahi S (2010). Application of vegetation indices for agricultural crop yield prediction using neural network techniques. Remote Sens. 2 (3), 673–696.

Picon A, Bereciartua-Perez A, Eguskiza I, Romero-Rodriguez J, Jimenez-Ruiz C J, Eggers T, Klukas C & Navarra-Mestre R (2022). Deep convolutional neural network for damaged vegetation segmentation from RGB images based on virtual NIR-channel estimation. *Artificial Intelligence in Agriculture*, *6*, 199–210. https://doi.org/10.1016/j.aiia.2022.09.004

Rabatel G, Gorretta N & Labbé S (2011). Getting NDVI spectral bands from a single standard RGB digital camera: A methodological approach. In *Advances in Artificial Intelligence* (pp. 333–342). Springer Berlin Heidelberg.

Rabatel G, Gorretta N & Labbé S (2014). Getting simultaneous red and near-infrared band data from a single digital camera for plant monitoring applications: Theoretical and practical study. *Biosystems Engineering*, *117*, 2–14. https://doi.org/10.1016/j.biosystemseng.2013.06.008

Rouse Jr, J W, Haas R H, Schell J A, Deering D W (1973). Monitoring the vernal advancement and retrogradation (green wave effect) of natural vegetation.

Sankaran S, Mishra A, Ehsani R, Davis C (2010). A review of advanced techniques for detecting plant diseases. Computers and Electronics in Agriculture, Volume 72, Issue 1, June 2010, Pages 1-13.

Sannier C A D, Taylor J C & Plessis W D (2002). Real-time monitoring of vegetation biomass with NOAA-AVHRR in Etosha National Park, Namibia, for fire risk assessment. *International Journal of Remote Sensing 23* (1): 71–89. https://doi.org/10.1080/01431160010006863

Thenkabail P S, Smith R B & De Pauw E (2000). Hyperspectral vegetation indices and their relationships with agricultural crop characteristics. *Remote Sensing of Environment*, *71*(2), 158–182. https://doi.org/10.1016/s0034-4257(99)00067-x

Trenn S (2008). Multilayer perceptrons: approximation order and necessary number of hidden units. *IEEE Transactions on Neural Networks*, *19*(5), 836–844. https://doi.org/10.1109/TNN.2007.912306

Wang L, Jin J, Song Z, Wang J, Zhang L, Rehman T U, Ma D, Carpenter N R & Tuinstra M R (2020). LeafSpec: An accurate and portable hyperspectral corn leaf imager. *Computers and Electronics in Agriculture*, *169* (105209), 105209. https://doi.org/10.1016/j.compag.2019.105209

Wang L, Duan Y, Zhang L, Rehman T, Ma D &Jin J (2020). Precise estimation of NDVI with a simple NIR sensitive RGB camera and machine learning methods for corn plants. Sensors (Basel, Switzerland), 20(11), 3208. https://doi.org/10.3390/s20113208

Xu H R, Ying Y B, Fu X P & Zhu S P (2007). Near-infrared spectroscopy in detecting leaf miner damage on tomato leaf. *Biosystems Engineering*, *96*(4), 447–454. https://doi.org/10.1016/j.biosystemseng.2007.01.008

Yang C M & Cheng C H (2001). Spectral characteristics of rice plants infested by brown planthoppers Proceedings of the National Science Council, Republic of China. *Part B, Life Sciences* 25(3): 180–186

Yang C M, Cheng C-H & Chen R-K (2007). Changes in spectral characteristics of rice canopy infested with brown planthopper and leaffolder. *Crop Science* 47(1): 329–335. https://doi.org/10.2135/cropsci2006.05.0335